ORIGINAL RESEARCH

Intralesional Axitinib Injection Mitigates Hypertrophic Scar by Inhibiting Angiogenesis Pathway: A Preliminary Study in a Rabbit Ear Model

Chuanbo Liu, Liang Tang, Chunsheng Hou, Jufang Zhang, Jinsheng Li

Department of Plastic and Cosmetic Surgery, Affiliated Hangzhou First People's Hospital, Zhejiang University School of Medicine, Hangzhou, Zhejiang, People's Republic of China

Correspondence: Jinsheng Li, Department of Plastic and Cosmetic Surgery, Affiliated Hangzhou First People's Hospital, Zhejiang University School of Medicine, No. 261, Huansha Road, Hangzhou, Zhejiang, 310006, People's Republic of China, Email 13567168364@126.com

Objective: High levels of VEGF and excessive angiogenesis contribute significantly to hypertrophic scar (HS) formation. Our study aimed to preliminarily investigate the effect of axitinib, a selective VEGF receptor tyrosine kinase inhibitor, on angiogenesis of HS and to explore its possible mechanism in a rabbit ear model.

Methods: Ten male New Zealand white rabbits were used to establish HS models and then randomised to the control and axitinib groups. The scar tissues in the two groups were injected with axitinib or normal saline, and they were evaluated after one month of treatment. Macroscopic scar thickness, vascularity and pliability, as well as histopathological analysis including HE staining and Masson staining and scar elevation index (SEI) between two groups were compared. Immunohistochemical staining of CD31 in two groups was conducted to assess the degree of angiogenesis in HS tissue. The protein expression of protein kinase B (AKT) and ribosomal protein S6 kinase (p70S6K) and their phosphorylation levels in both groups were examined by Western blot analysis.

Results: The macroscopic and histological observation showed intralesional axitinib injection significantly reduced scar thickness, vascularity and pliability of HS in the rabbit ear model. The value of SEI in HE assessment was also significantly declined in the axitinib group. Furthermore, immunohistochemical analysis revealed that axitinib suppressed the expression of CD31 in HS tissue, and the mean IOD for blood vessels was significantly lower in the axitinib-treated group. Additionally, axitinib effectively attenuated the protein expression of p70S6K, p-AKT and p-p70S6K by Western blot analysis.

Conclusion: Our study suggests that intralesional injection of axitinib can effectively attenuate HS by reducing angiogenesis in the rabbit ear model, and this inhibitory effect may be mediated by suppression of AKT/p70S6K signaling pathway. It indicates that axitinib may be a promising option for the treatment of HS in the future.

Keywords: hypertrophic scar, axitinib, angiogenesis, rabbit ear scar model

Introduction

Hypertrophic scar (HS) is a difficult clinical challenge to tackle with. HS usually develops following burns, trauma or surgery, and it is characterized with disorganized structure and abnormal biomechanical property.[1] It frequently causes aesthetic issues, itching, and pain, restricts mobility of the joints, impairs tissue growth and even leads to psychosocial consequences. HS can significantly reduce the quality of life for patients, there is yet a lack of standardized antiscar protocol to date. Each of the current therapies including silicone gel,[2] laser treatment,[3,4] steroid injection,[5] radiotherapy,[6] and surgical operation[7] highlights a certain stage in the complex process of HS formation based on the underlying molecular mechanisms.[6] Therefore, it is necessary to explore new potential therapeutic strategies that target on the specific factors involved in scar formation to minimize the appearance of HS.

Angiogenesis is an extremely sophisticated process that plays a critical role in wound repair and tissue regeneration.[8,9] The angiogenic processes of wound healing is regulated by a variety of factors, and one particularly potent proangiogenic mediator is vascular endothelial growth factor (VEGF).[10,11] VEGF is a 40–45 kDa heterodimeric glycoprotein, and it consists of

a family of several members including VEGF-A, VEGF-B, VEGF-C, VEGF-D, VEGF-E, VEGF-F, placenta growth factor (PlGF) and endocrine gland-derived vascular endothelial growth factor (EG-VEGF).[11] VEGF binds to different VEGF Tyrosine Kinase Receptors (VEGFRs) such as VEGFR-1 (flt-1), VEGFR-2 (flk-1) and VEGFR-3 (flt-4), and then activates several intracellular signaling pathways to stimulate mitogenesis and inhibit apoptosis in vascular endothelial cells.[11–13] VEGF-VEGFRs-induced downstream signaling pathways via protein kinase B (PKB, widely known as AKT) and extracellular signal regulated kinase (ERK) regulate cell proliferation, promote cell migration, stimulate cell survival, increase vascular permeability, and form capillary tube, thereby significantly influencing angiogenesis in the process of HS formation.[11,13–16] Despite the essential role of angiogenesis in wound healing, more evidences[8,17] have confirmed that high levels of VEGF and excessive neovascularization contribute to HS production. Therefore, inhibiting angiogenesis induced by VEGF and its receptors is a potent element in HS therapy and management.

Anti-VEGF-VEGFRs agents, which inhibit VEGF or its receptors, are currently being applied or tested to suppress angiogenesis in the therapy of certain cancers and ophthalmic diseases.[18,19] Several tyrosine kinase receptors such as sorafenib[20] and sunitinib[21] to block the cascade of VEGFRs signal transduction have been approved for the treatment of solid tumors by US Food and Drug Administration. Given the crucial role of VEGF-VEGFRs signaling in the development of HS formation, these anti-VEGFR small molecular drugs could be possibly employed to reduce scar tissue deposition in clinic. What is more, a series of experimental and clinical researches[13,22] have established that anti-VEGFRs agents can prevent or treat scar tissue.

Axitinib (AG-013736) is a small molecular inhibitor that selectively targets VEGFRs to suppress angiogenesis.[16,23] It is currently being considered as an alternative drug for various types of malignant carcinomas.[23,24] Due to its high selectivity to VEGFRs and relatively short half-life,[23] axitinib has the potential to become a potent and safe medicine with fewer side effects and greater tolerability in clinical settings. Therefore, we speculate that administration of axitinib may also have a therapeutic effect on HS tissue. To the best of our knowledge, no published studies have been conducted to assess the antiangiogenic effects of intralesional axitinib injection on established HS. Thus, our study attempted to preliminarily elucidate whether local injection of axitinib can attenuate HS by suppressing angiogenesis and explore the possible mechanisms involved in the rabbit ear model.

Methods and Materials

The experimental protocol was approved by the Ethics Committee of Affiliated Hangzhou First People's Hospital, Zhejiang University School of Medicine, and conducted in accordance with Guide for the Care and Use of Laboratory Animals (National Research Council, 2011, Eighth Edition). The animal experiment and molecular biological detection were conducted between June 2022 and March 2023. Ten healthy male adult New Zealand white rabbits, aged 4–5 months and with an average weight of 2.8 kg, were purchased from Xinjian Rabbit Farm of Xinchang County, Zhejiang Province. All animals were housed individually and maintained according to current standards of animal experiments.

Establishment of the Rabbit Ear HS Model

The rabbit ear model of HS was established according to the previously described procedure with a minor modification.[25,26] Briefly, anesthesia was induced by injecting propofol (15mg/kg) through the auricular vein, and afterwards anesthesia was maintained using isoflurane in all rabbits. Four circular wounds, each with a diameter of 15 mm, were then created on the ventral surface of each ear using a biopsy punch under aseptic conditions as indicated in Figure 1A. The complete removal of skin, subcutaneous tissues and perichondrium in each wound was required, and 80 full-thickness wounds in ten rabbits were created in total. Pressure was applied to control bleeding, and the wounds were left exposed to the air. Daily wound examination and care were performed until complete healing was achieved.

In our rabbit ear model of HS, wound closure began on the 7th day following the surgical procedure and was complete by the 14th day. At 30th day after operation, a significantly raised scar tissue was formed as illustrated in Figure 1B. The HS model in a rabbit ear was confirmed through macroscopic and histological analysis as shown in Figure 1C and D.
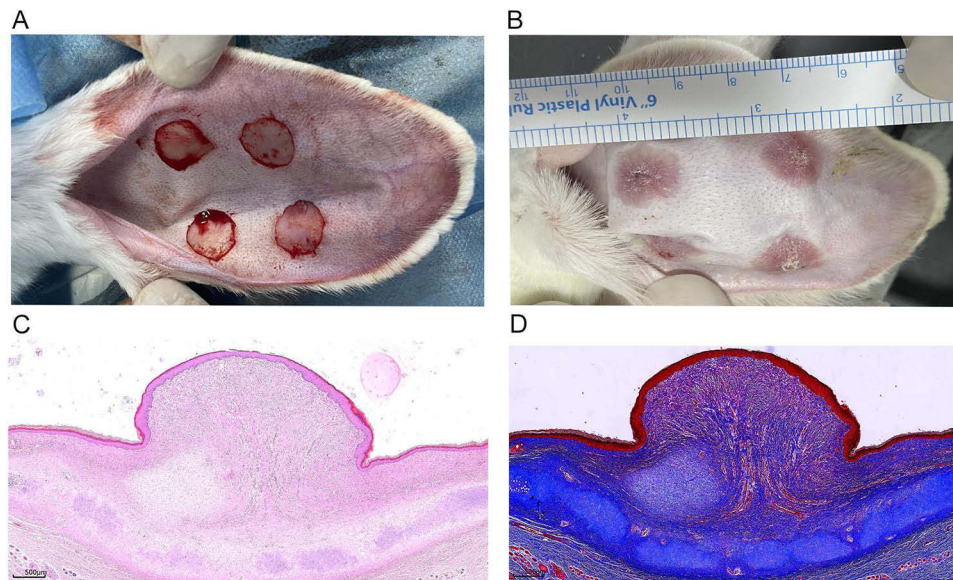
Figure 1 Hypertrophic scar (HS) was established in a rabbit ear. (**A**) Four 15 mm-diameter circular wounds were created on the ventral surface of each ear by removal of tissue deep to the perichondrium. (**B**) The gross view of HS in the rabbit ear was observed at 30th day after operation. (**C** and **D**) The histopathological appearance of HS was shown by HE staining (×25) and Masson staining(×25) respectively.

Preparation and Usage of Axitinib

Axitinib (AG-013736) was purchased from Selleck Chemicals LLC (Houston, USA), and stored in a refrigerator at −20 °C away from light until it was dissolved.

Unfortunately, there is not yet a reference article about the experimental approaches of axitinib in the field of scar research. The appropriate concentration of axitinib for local injection to scar lesions was unknown, as it is typically used as oral administration for solid tumors[24] or as ophthalmic drops for corneal neovascularization.[27] Therefore, a concentration of 1.25mg/mL for intra-scar injection was formulated based on preliminary experiments and referencing drug concentrations for both modes of administration. The solution was kept at −20°C refrigerator until use.

Experimental Protocol in Different Groups

The HS model was established and confirmed on day 30 post-wounding. Ten rabbits were then randomly assigned to either the axitinib group or the control group, with five rabbits and forty scars in each group. Thus, five rabbits including forty scar tissues in each group initiated to receive therapy. Each scar in the axitinib group was treated intra-lesionally with 200ul of axitinib using an 1mL syringe needle, while every scar in the control group was injected with an equal volume of normal saline. The treatment was administered to the established scar once per week for a duration of two weeks. Sufficient solution (200ul) was used to blanch each entire scar tissue, and the two injections were carried out from the same location. After one month from the initiation of treatment, all rabbits were humanely sacrificed with euthanasia through an anaesthesia overdose. The gross appearance of scar tissues in both groups was photographed and recorded. Furthermore, all scars were harvested for histological examination and Western blot analysis.

Gross Evaluation of HS

The macroscopic appearance of HS was compared between the axitinib group and the control group through visual observation. To accurately assess the differences in scar characteristics between the two groups, scar thickness (cm) was measured using a vernier caliper. In addition, scar vascularity and pliability were evaluated using the Vancouver Scar Scale (VSS),[28] an extensively applied tool for scar tissue assessment. Scar vascularity was scored on a scale of 0 to 3, with normal being 0, pink being 1, red being 2, and purple being 3. Scar pliability was scored on a scale of 0 to 5, with normal being 0, supple being 1, yielding being 2, firm being 3, banding being 4, and contracture being 5.

These indicators, including scar thickness, vascularity and pliability, were assessed in real time as the animals were euthanised. This evaluation was performed in a blinded fashion, with the assessor unaware of the treatment of the scar tissue.

Histopathological Assessment of HS

The histopathological comparison of HS between the axitinib group and the control group was evaluated using haematoxylin and eosin (HE) staining and Masson staining.

The scar specimens were fixed in 4% paraformaldehyde solution, embedded in paraffin, and cut into sections at a thickness of 4 μm. The slices of scar tissue were processed with HE staining to assess the morphological changes of scar tissue after treatment. What is more, the sections of scar tissue were stained with Masson to evaluate the collagen fiber arrangement, and collagen volume fraction (CVF) was analyzed quantitatively to compare collagen expression between two groups. CVF was measured as the percentage of collagen area (dyed with blue) divided by the total scar tissue area using Image-Pro software.

Scar elevation index (SEI)[25] was measured using HE stained tissue slides to objectively evaluate the degree of scar hyperplasia. SEI was calculated as the ratio of the maximum height of the scar to that of the surrounding normal skin, and the value of existed HS was defined as >1.0. Specifically, the height was gauged perpendicularly between the highest point of scar/skin tissue and the surface of auricular cartilage by an Image-Pro software version 6 (Media Cybernetics, Maryland, USA).

Immunohistochemical Staining and Analysis of CD31 Expression

Immunohistochemical staining of CD 31 was conducted to assess the degree of angiogenesis[29] in HS tissue.

The sections of scar tissue were dewaxed and subjected to microwave-assisted EDTA repair solution. The sections were then treated with 3% hydrogen peroxide for 10 minutes to eliminate endogenous peroxidase activity. After washing with PBS, the slides were blocked with 5% bovine serum albumin (BSA) for 30 minutes. The slides were then incubated with anti-rabbit CD31 primary antibody (Proteintech, Wuhan, China) overnight at 4 °C. Following washes with PBS, the slides were incubated with goat anti-rabbit IgG/HRP antibody (ZSGB bio, Beijing, China) for 30 minutes at 37°C. The slides were incubated with DAB, counterstained with hematoxylin and finally sealed. CD31 expression was analyzed at ×400 magnification using Image-Pro software 6, and CD31 positivity was defined as the presence of brownish-yellow granules in vascular endothelial cells in the sections. The mean integrated optical density (IOD) was calculated by dividing the IOD by the area of each image, and the mean IOD of each section was obtained by measuring 5 random areas.

Protein Extraction and Western Blot Analysis

The HS specimens from ten rabbits for Western blot assessment were frozen in liquid nitrogen and stored in a refrigerator at −80 °C.

The scar tissues were weighed, and protein was extracted using RIPA lysis buffer (KeyGEN BioTECH, Nanjing, China). The protein concentration was determined with a BCA Protein Assay Kit (KeyGEN BioTECH, Nanjing, China) using Microplate Reader at a wavelength of 562nm. Afterwards, protein samples (30 μg total protein per lane) were loaded onto a vertical sodium dodecyl sulfate- polyacrylamide gel electrophoresis (SDS-PAGE) system. Following electrophoresis using SDS-PAGE, protein samples were separated and then transferred to nitrocellulose (NC) membrane (GE Healthcare, Amersham, UK).

NC membrane was blocked with skim milk powder at room temperature for one hour, and then incubated at 4°C overnight with primary antibodies: anti-β-actin (Santa Cruz, CA, US), anti-AKT (Santa Cruz, CA, US), anti-p70 S6K (Santa Cruz, CA, US), anti-phospho-AKT (Cell Signaling Technology, Danvers, US) and anti-phospho-p70 S6K (Santa Cruz, CA, US). After washing with TBST, the NC membrane was incubated at room temperature for one hour with secondary antibodies: horseradish peroxidase (HRP)-labeled goat anti-rabbit IgG (Kirkegaard & Perry Laboratories, Inc., Gaithersburg, US). Protein bands were visualised using enhanced chemiluminescent (ECL) (SuperSignal West Femto Maximum Sensitivity Substrate, Thermo Fisher Scientific, Carlsbad, US), and analyzed by Amersham Imager 680 (AI 680) program (GE Healthcare, Amersham, UK).

Statistical Analysis

Statistical analysis was carried out by SPSS software version 20, and statistical chart was performed with GraphPad Prism software version 8. The descriptive statistics results were expressed as the mean ± standard deviation. The comparison of scar height, scar scores of vascularity and pliability, SEI, mean IOD for blood vessels, and the expression of AKT, p-AKT, p70S6K and p-p70S6K between the control group and the axitinib group were analyzed using the *t*-test for two independent samples. The value of $P < 0.05$ was regarded as statistically significant.

Results

The Rabbit Ear HS Model Was Confirmed from Both Macroscopic and Histological View

According to gross observation through vision, the wounds started to close at 7th day after the operation and were completely healed by 14th day after operation. At 30th day after the surgical procedure, a significant HS was formed as depicted in Figure 1B. The established scars at the injury sites were distinctly elevated above the plane of circumambient undamaged normal skin, and the thickness of scars was almost twice that of normal skin. The scars appeared dark red in color and had a hard texture.

Upon histological observation under a light microscope, it was found that the epidermal layer of scars remained intact, while the dermal layer exhibited a significant thickening, which was in accordance with the findings from gross view. HE staining (refer to Figure 1C) demonstrated denser and disarranged collagen fibers, as well as massive infiltrated fibroblasts and microvascular hyperplasia in the dermis of scars. Masson staining (refer to Figure 1D) similarly revealed a large number of disordered and blue-dyed collagen fiber hyperplasia.

From the Perspective of Gross Evaluation, Axitinib Significantly Reduced Scar Thickness, Vascularity and Pliability of HS in a Rabbit Ear Model

As shown in Figure 2A and B, the HS tissue in the axitinib group was less noticeable and more similar in appearance to normal skin compared to that in the control group. From gross view, the scar thickness decreased significantly, its texture became softer, and its color faded in the axitinib-treated group.

Quantitative and semi-quantitative indicators including scar thickness, vascularity and pliability were used to accurately evaluate scar differences between the two groups. The scar height in the axitinib group was significantly lower than that in the control group (2.8 ± 0.5cm vs 3.4 ± 0.7cm, $P < 0.01$) as shown in Figure 2C. Additionally, the scar scores of vascularity (1.5 ± 0.7 vs 2.2 ± 0.7, $P < 0.01$) and pliability (1.6 ± 0.8 vs 2.4 ± 0.7, $P < 0.01$) in axitinib-treated group were both reduced compared to those in the control group (Figure 2D and E).

Furthermore, no adverse effects such as allergy, erythema, erosion or dyspigmentation were observed in the HS of rabbit ears with intra-scar axitinib injection.

These results suggested that axitinib could mitigate HS in a rabbit ear model from a gross perspective, and intralesional injection of axitinib is potentially safe and feasible for the treatment of HS in rabbit ears.

In Terms of Histopathological Evaluation, Axitinib Inhibited Histologic Changes in a Rabbit Ear HS Model

Compared with the control group (Figure 3A and C), the dermal layer of scars in the axitinib group (Figure 3B and D) was significantly thinner, with prominently decreased collagen deposition and collagen fibers arranged in a relatively less irregular manner that tended to be parallel to the skin. Furthermore, the number of fibroblasts and microvessels in the axitinib group was remarkably subsided in HE staining (Figure 3B and D). Masson staining showed the same result that the density of blue-dyed collagen fibers was decreased and the arrangement of collagen bundle was in a more regular order in the axitinib group (Figure 4B and D) when compared with that in the control group (Figure 4A and C). Quantitative collagen analysis also showed that the CVF value (%) was significantly reduced in the axitinib group (47.4 ± 6.3 vs 71.1 ± 4.5, $P < 0.01$) (Figure 4E).

Additionally, SEI was calculated in HE staining to further confirm the effect of axitinib injection on the established HS. The value of SEI in the axitinib group was significantly declined than that in the control group (1.9 ± 0.4cm vs 2.8 ± 0.6cm, $P < 0.01$) (Figure 5).
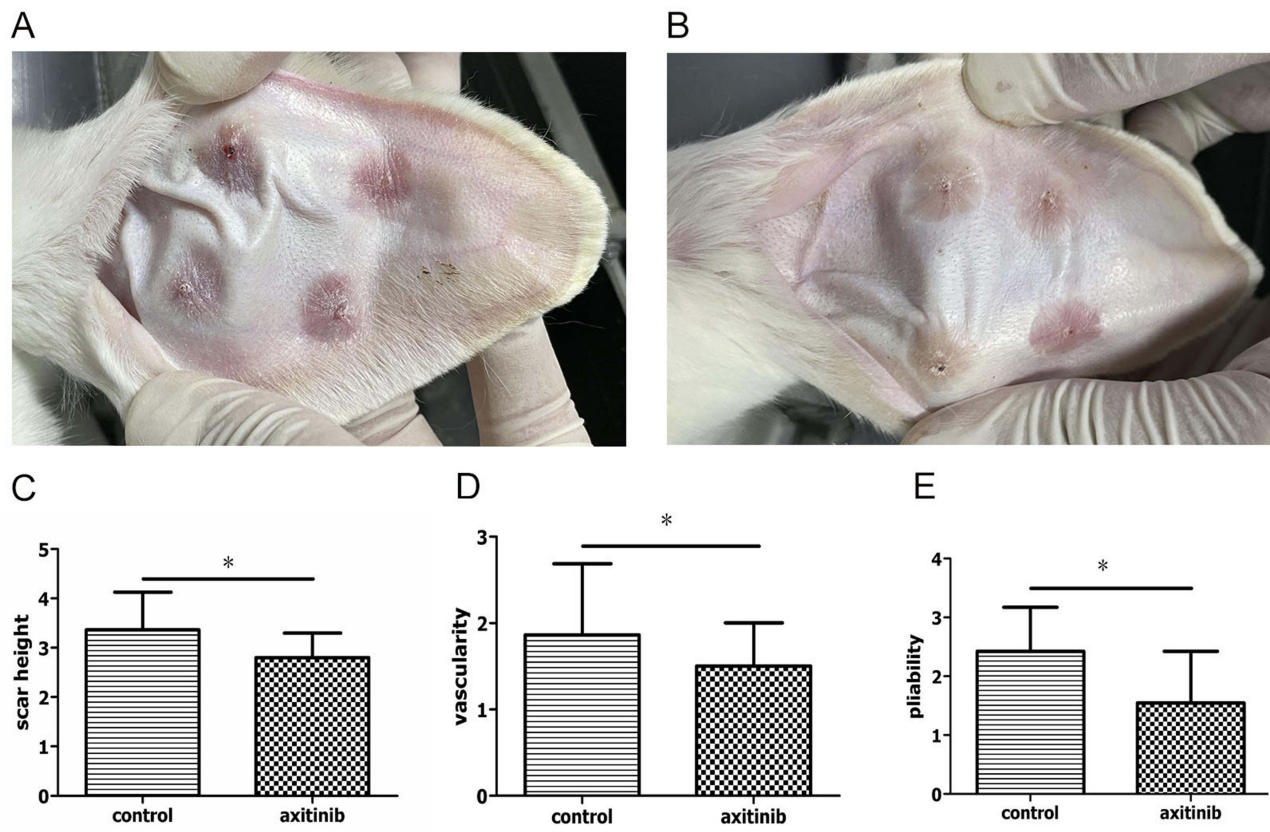
Figure 2 The inhibitory effect of axitinib on HS in a rabbit ear was observed from gross view. (**A** and **B**) The scar tissue was less conspicuous in axitinib group (**B**) than that in control group (**A**). (**C**–**E**) In comparison with HS in the control group, scar thickness (**C**), vascularity (**D**) and pliability (**E**) of HS was significantly decreased in the axitinib group (n = 40 per group). *$P < 0.05$.
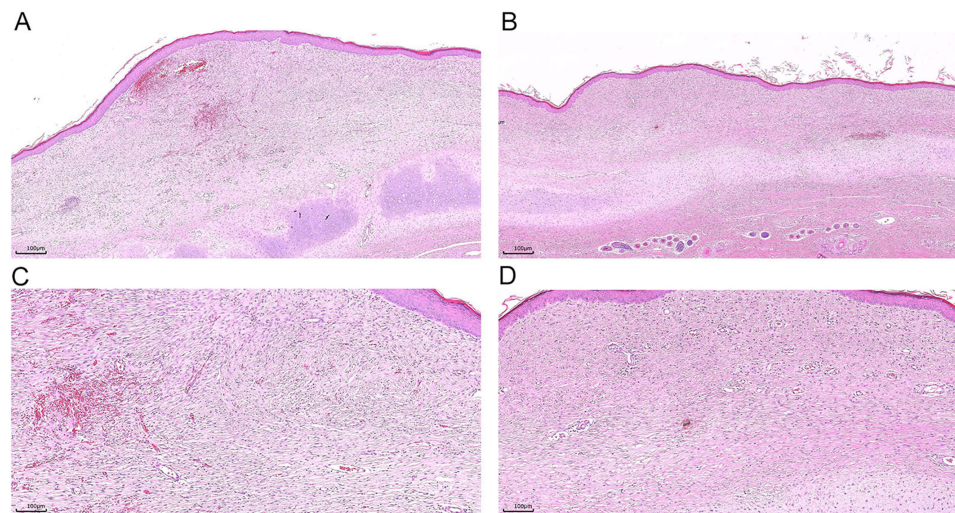

Figure 3 Histopathological images of HE stained HS after treatment. Compared to the control group ((**A**), ×40, (**C**), ×100, n = 20), the axitinib group showed decreased and relatively less organised collagen, and reduced fibroblasts and microvessels ((**B**), ×40, (**D**), ×100, n = 20).

These results further reaffirmed that axitinib could alleviate established HS in a rabbit ear model from a histological perspective.
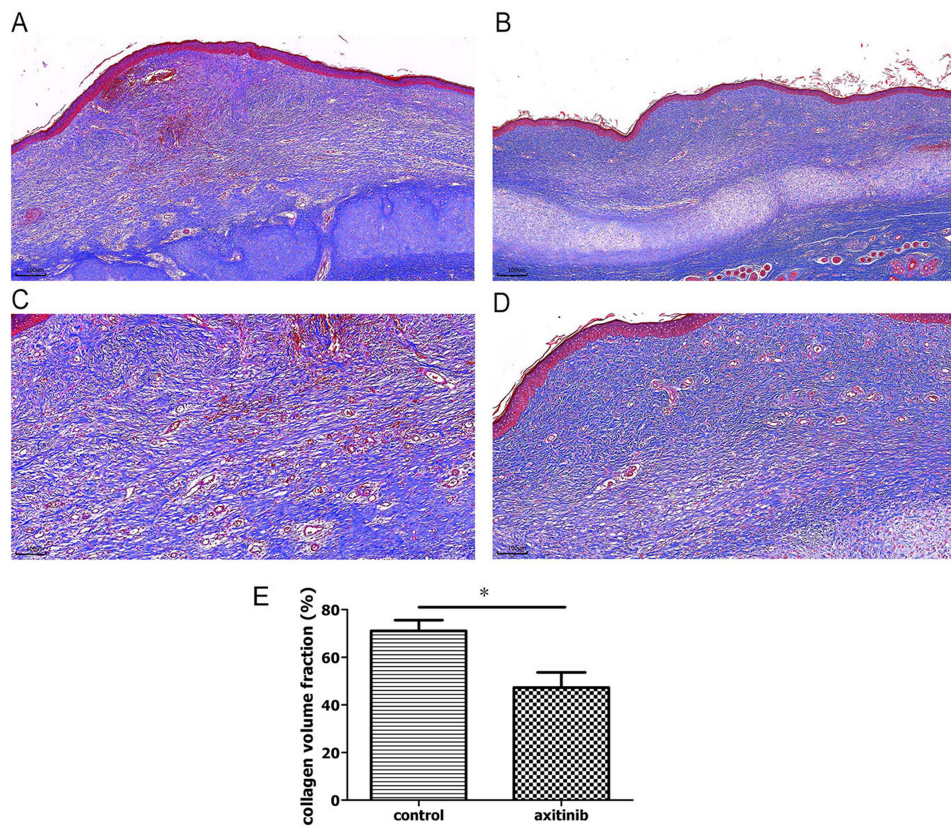
Figure 4 Histopathological images of Masson stained HS after treatment. (**A–D**) In contrast with that in the control group ((**A**), ×40, (**C**), ×100, n = 20), collagen fibers were loose and regularly arranged in the axitinib group ((**B**), ×40, (**D**), ×100, n = 20). (**E**) The value of collagen volume fraction (CVF, %) was significantly decreased in the axitinib group (n = 20 per group). *P < 0.05.
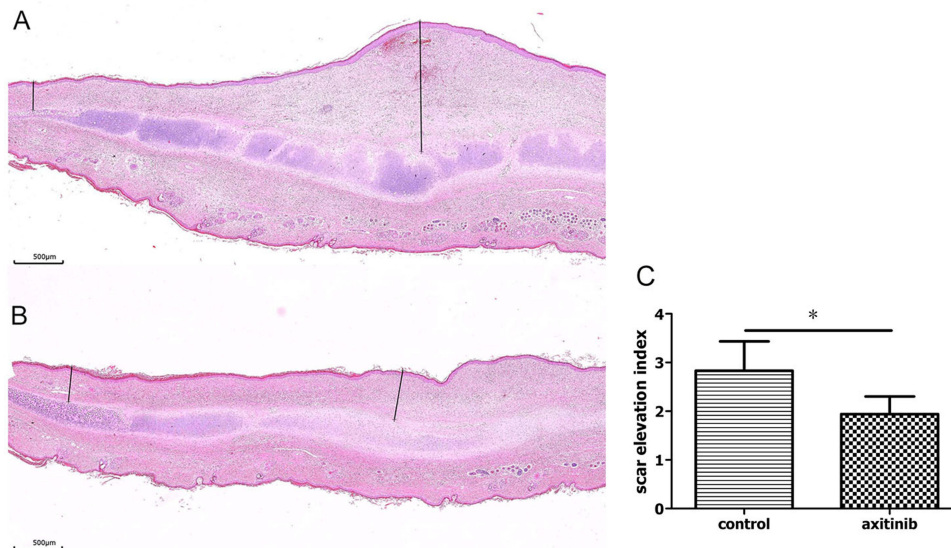

Figure 5 Scar elevation index (SEI) in HE analysis of HS after treatment. (**A** and **B**) SEI was calculated in HE staining (×25) between two groups by the ratio of the maximum height of scar to that of surrounding normal skin. (**C**)The value of SEI was significantly decreased in the axitinib group (n = 20 per group). *P < 0.05.

Axitinib Suppressed CD 31 Expression, a Key Marker of Angiogenesis, in a Rabbit Ear HS Model

HS tissues from two groups were stained with anti-CD31 antibody for immunochemical detection of blood vessels. The expression of CD31 in vasculature (×200, ×400) was lower in the axitinib group (Figure 6B and D) than that in the control group (Figure 6A and C). The mean IOD for blood vessels was used to further quantitatively analyze angiogenesis of scar tissue in different groups, and it discovered that the mean IOD was significantly lower in the axitinib-treated group (0.03 ± 0.001 vs 0.07 ± 0.016, $P = 0.010$) (Figure 6E).

These results confirmed that axitinib effectively suppressed angiogenesis of HS in a rabbit ear model.

Axitinib Attenuated the Expression of Ribosomal Protein S6 Kinase (p70S6K), p-AKT and p-p70S6K, Critical Downstream VEGF-VEGFR Signaling Molecules in a Rabbit Ear HS Model

The expression of AKT and p70S6K, the phosphorylation levels of AKT and p70S6K were examined by Western blot. The results shown in Figure 7A displayed that the expression of β-actin was consistent across all groups. The expression levels of p-AKT, p70S6K and p-p70S6K in the axitinib group were all remarkably reduced than that in the control group.

Subsequently, the relative levels of AKT, p-AKT, p70S6K, and p-p70S6K were quantified using the ratios of AKT/β-actin, p-AKT/β-actin, p70S6K/β-actin, and p-p70S6K/β-actin, respectively, for further quantitative analysis. As revealed in Figure 7C, D, and E, the relative levels of p-AKT (1.4 ± 0.4 vs 0.6 ± 0.3, $P < 0.01$), p70S6K (1.4 ± 0.6 vs 0.6 ± 0.4, $P < 0.05$) and p-p70S6K (1.5 ± 0.4 vs 0.6 ± 0.3, $P < 0.01$) in the axitinib group were significantly lower than that in the control group.

However, the expression levels of AKT between two groups were similar, and there was no significant difference in the relative levels of AKT (1.1 ± 0.4 vs 1.0 ± 0.5, $P > 0.05$) as displayed in Figure 7A and B.
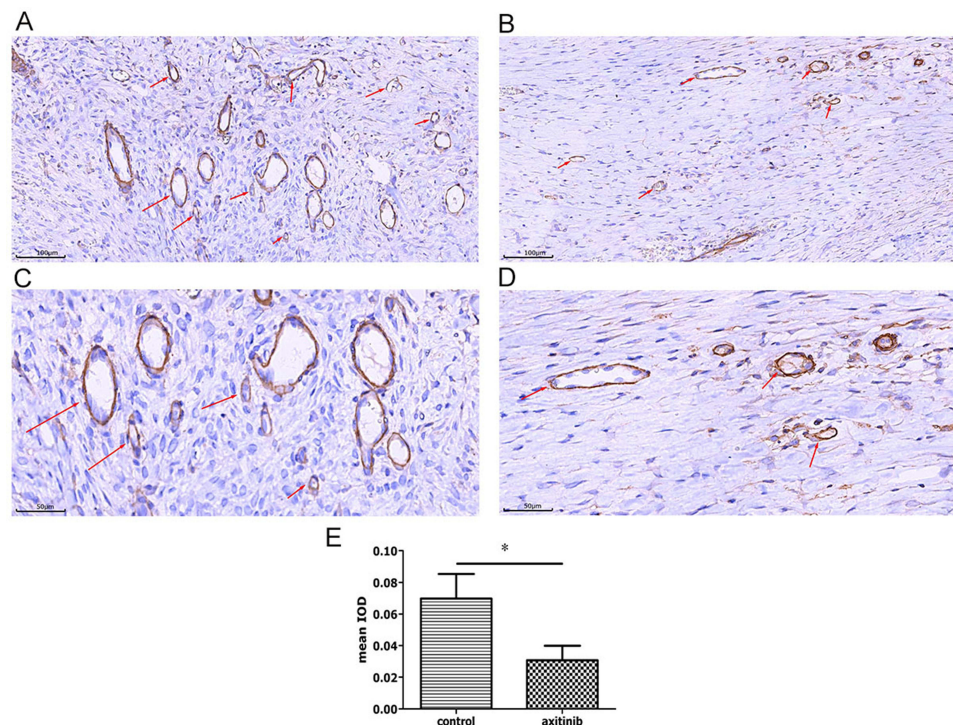

Figure 6 Axitinib inhibited HS angiogenesis. (**A–D**) Expression of CD31 (as shown by red arrows) in immunohistochemical staining of scar tissues from two groups. CD31 was less in the axitinib group ((**B**), ×200, (**D**), ×400) than that in the control group ((**A**), ×200, (**C**), ×400). (**E**) Mean IOD for blood vessels between two groups analyzed by Image-Pro Plus 6. The difference in mean IOD between two groups was significant (n = 20 per group, P = 0.010). *P < 0.05.

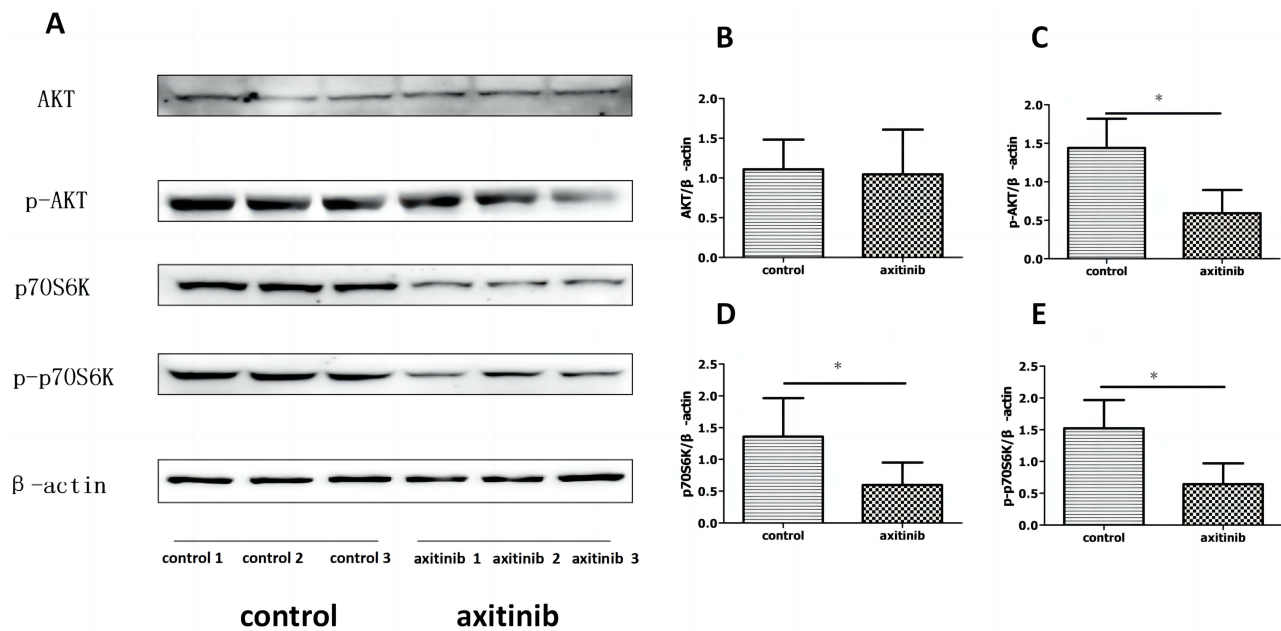**Figure 7** Axitinib significantly reduced levels of p-AKT, p70S6K and p-p70S6K shown in Western blot results. (**A**) The protein levels of AKT and p-AKT, p70S6K and p-p70S6K were determined by immunoblot (n = 6 per group). (**B**) No significant difference in the relative levels of AKT was detected (P > 0.05). (**C–E**) The relative levels of p-AKT (**C**), p70S6K (**D**) and p-p70S6K (**E**) in the axitinib group were significantly lower than that in the control group (P < 0.05). *P < 0.05.

These results of protein expression analysis indicated that intralesional injection of axitinib significantly suppressed the expression of p-AKT, p70S6K and p-p70S6K in HS tissues of a rabbit ear model.

Discussion

HS is a challenging clinical problem, particularly in the Asian population.[30] The pathogenesis of HS is complicated and not yet fully understood.[6,9] Various therapeutic methods such as silicone gel or sheet, steroid injection, laser therapy, surgical repair, or a combination of these above mentioned methods are currently employed for the prevention and treatment of HS.[2–4,7,30] However, these treatment approaches have drawbacks including scar recurrence and systemic adverse reactions,[7,30] and there is still short of effective antiscar remedies at present. Because of the psychological and functional hazards caused by HS, it is urgent to find new therapeutic solutions to improve the patients' quality of life and psychological well-being.[6] Our study preliminarily confirmed that intralesional injection of axitinib can significantly attenuate HS tissue in a rabbit ear model by suppressing angiogenesis through the AKT/p70S6K pathway. This is the first evidence of local axitinib injection in HS therapy, suggesting that axitinib may be a promising treatment option for HS.

Axitinib (AG-013736), one of anti-angiogenic agents that block VEGFRs, is a potent and selective inhibitor of VEGF receptor tyrosine kinases 1, 2 and 3, and it has been applied in the current clinical treatment of certain solid tumors.[18,23,24] Because angiogenesis plays a crucial role in the development and progression of some pathophysiological conditions including cancers and HS,[11,18] we hypothesized that axitinib might also be used in the therapy of HS by suppressing angiogenesis. In order to verify the potential effects of axitinib in the treatment of HS, the rabbit ear model of HS was designed. Despite some limitations, the rabbit ear HS model remains one of the most widely used methods for researching scar pathogenesis and therapy.[26]

Axitinib was originally orally administrated for cancer treatment[31] or topically used for corneal neovascularization.[27] Although axitinib can be used in various formulations for the clinical and experimental treatment, systemic administration of axitinib may have some side effects and thus restrict its clinical application.[16,23] Therefore, local injection of axitinib into scar tissue was adopted in this study. However, no study has been conducted to explore the effect of axitinib on the rabbit ear HS model, and the concentration of axitinib injected into the scar was still unknown. Taking into account the difference between

skin and corneal tissue, skin is more durable than intraocular tissue.[32] The injection concentration of axitinib in our experiment was identified at 1.25mg/mL, which was higher than the concentration of axitinib eye drops for ocular diseases.[27]

Our study showed that intralesional injection of axitinib mitigated scar hyperplasia in the rabbit ear HS model. The result is consistent with the inhibitory effect of other anti-angiogenic drugs, such as bevacizumab,[32] usnic acid,[33] and endostatin,[34] which have been shown to be effective in modulating scar in previous studies. In the view of gross anatomy, the scar was less visible and its aesthetic appearance was significantly improved. To be specific, scar thickness, erythematous coloration and pliability were decreased with local injection of axitinib. Both HE and Masson staining from the perspective of histopathology further confirmed that collagen density was decreased and collagen arrangement was in a more regular order in the axitinib-treated group. What is more, the declined SEI value in HE staining evaluation reaffirmed that topical axitinib injection reduced scar thickness. In addition, there were no observed adverse effects, including allergies, erythema, erosion, or dyspigmentation, in the HS tissue of rabbit ears following application of axitinib. These results hint that axitinib injection is potentially safe and feasible for the treatment of HS in rabbit ears.

It has been well established that angiogenesis plays a vital role in the process of HS formation.[1,11] VEGF acts as a significant proangiogenic factor in the complex neovascular process, and several angiogenesis inhibitors targeting VEGF-VEGFRs have been elucidated to effectively prevent and treat scars.[32–34] Some studies have revealed that blockade of VEGF-VEGFRs signaling resulted in inhibition of angiogenesis through suppression of the endothelial nitric oxide synthase (eNOS), AKT and ERK pathway cascades.[11,12,14–16,35] In particular, phosphoinositide-3-kinase (PI3K), AKT, mTOR, and p70S6K are critical downstream signaling molecules in the AKT pathway.[12,16,35] Our study revealed the ability of axitinib injection to suppress HS, as evidenced by macroscopic and pathological scar morphological changes after treatment. What is more, our team sought to further confirm whether the inhibitory effect of axitinib on HS was related to the suppression of AKT signal transduction. Molecular biology techniques in this experiment were then employed to investigate the possible mechanisms underlying its suppressive effect. The diminished expression of CD31, a significant marker of angiogenesis,[29] in immuno-histochemical analysis of our research revealed that angiogenesis was obviously reduced in HS tissue section using axitinib. Western blot analysis conducted in this study further found that axitinib injection effectively inhibited the expression of p70S6K, p-AKT and p-p70S6K, although the levels of AKT were not significantly different. These results clarified that local axitinib injection could effectively inhibited HS in the rabbit ear model by suppressing angiogenesis, and the potential mechanism may be associated with AKT/p70S6K pathway cascades.

Our study provides some references on concentrations, duration and molecular mechanisms for potential clinical applications of axitinib injection for HS treatment. There are still some limitations and deficiencies in our study. First, there was no positive control in our study, and only one concentration of intra-scar axitinib injection was validated effective in reducing HS. Since triamcinolone is a first-line medication for scar treatment in clinical practice, and the appropriate concentration of axitinib injection for scar therapy was unknown in previous studies, the usage of positive control (triamcinolone) and different concentrations of axitinib in two or more groups were better to get a more convincing result. Further researches should investigate the optimum concentration of axitinib to minimize HS while not delaying the wound healing process. Second, this study confirmed the efficacy and safety of intra-scar axitinib injection in HS treatment and the possible mechanism only in the rabbit ear model. These signaling pathway proteins need to be reaffirmed in endothelial cells of scar tissue in vitro with special inhibitors. Third, the efficiency and toxicity of axitinib on HS were relatively short, and long-term effects remain to be examined in the future.

In conclusion, our study indicates that the intralesional injection of axitinib can attenuate HS by reducing angiogenesis in the rabbit ear model, and this inhibitory effect of axitinib may be mediated by suppression of AKT/p70S6K pathway cascades. To the best of our knowledge, this is the first study to preliminarily investigate axitinib injection in the treatment of HS and its potential mechanisms. Therefore, axitinib may be a potential option for the treatment of HS alone or in combination with other therapies in the future. However, additional researches should be conducted to reveal the therapeutic mechanism, and more studies will be needed to further determine the optimal usages and dosages of axitinib to achieve the best therapeutic effect and to avoid significant side events.

Funding

Disclosure

The authors report no conflicts of interest in this work.

References

1. Lee HJ, Jang YJ. Recent understandings of biology, prophylaxis and treatment strategies for hypertrophic scars and keloids. *Int J Mol Sci*. 2018;19 (3):1. doi:10.3390/ijms19030711
2. Hsu KC, Luan CW, Tsai YW. Review of silicone gel sheeting and silicone gel for the prevention of hypertrophic scars and keloids. *Wounds*. 2017;29(5):154–158.
3. Seago M, Shumaker PR, Spring LK, et al. Laser treatment of traumatic scars and contractures: 2020 international consensus recommendations. *Lasers Surg Med*. 2020;52(2):96–116doi:10.1002/lsm.23201
4. Lv K, Liu H, Xu H, et al. Ablative fractional CO(2) laser surgery improving sleep quality, pain and pruritus in adult hypertrophic scar patients: a prospective cohort study. *Burns Trauma*. 2021;9:tkab023. doi:10.1093/burnst/tkab023
5. Ledon JA, Savas J, Franca K, Chacon A, Nouri K. Intralesional treatment for keloids and hypertrophic scars: a review. *Dermatol Surg*. 2013;39 (12):1745–1757. doi:10.1111/dsu.12346
6. Mony MP, Harmon KA, Hess R, Dorafshar AH, Shafikhani SH. An updated review of hypertrophic scarring. *Cells*. 2023;12(5):678. doi:10.3390/cells12050678
7. Ogawa R. The most current algorithms for the treatment and prevention of hypertrophic scars and keloids: a 2020 update of the algorithms published 10 years ago. *Plast Reconstr Surg*. 2022;149(1):79e–94e. doi:10.1097/PRS.0000000000008667
8. DiPietro LA. Angiogenesis and wound repair: when enough is enough. *J Leukoc Biol*. 2016;100(5):979–984. doi:10.1189/jlb.4MR0316-102R
9. Gurtner GC, Werner S, Barrandon Y, Longaker MT. Wound repair and regeneration. *Nature*. 2008;453(7193):314–321. doi:10.1038/nature07039
10. Ogawa R, Akaishi S. Endothelial dysfunction may play a key role in keloid and hypertrophic scar pathogenesis - Keloids and hypertrophic scars may be vascular disorders. *Med Hypotheses*. 2016;96:51–60. doi:10.1016/j.mehy.2016.09.024
11. Wilgus TA. Vascular endothelial growth factor and cutaneous scarring. *Adv Wound Care*. 2019;8(12):671–678. doi:10.1089/wound.2018.0796
12. Song Y, Dai F, Zhai D, et al. Usnic acid inhibits breast tumor angiogenesis and growth by suppressing VEGFR2-mediated AKT and ERK1/2 signaling pathways. *Angiogenesis*. 2012;15(3):421–432. doi:10.1007/s10456-012-9270-4
13. Wilgus TA, Ferreira AM, Oberyszyn TM, Bergdall VK, Dipietro LA. Regulation of scar formation by vascular endothelial growth factor. *Lab Invest*. 2008;88(6):579–590. doi:10.1038/labinvest.2008.36
14. Tanimoto T, Jin ZG, Berk BC. Transactivation of vascular endothelial growth factor (VEGF) receptor Flk-1/KDR is involved in sphingosine 1-phosphate-stimulated phosphorylation of Akt and endothelial nitric-oxide synthase (eNOS). *J Biol Chem*. 2002;277(45):42997–43001. doi:10.1074/jbc.M204764200
15. Shiojima I, Walsh K. Role of Akt signaling in vascular homeostasis and angiogenesis. *Circ Res*. 2002;90(12):1243–1250. doi:10.1161/01.RES.0000022200.71892.9F
16. Gao L, Nadora DM, Phan S, et al. Topical axitinib suppresses angiogenesis pathways induced by pulsed dye laser. *Br J Dermatol*. 2015;172 (3):669–676. doi:10.1111/bjd.13439
17. DiPietro LA. Angiogenesis and scar formation in healing wounds. *Curr Opin Rheumatol*. 2013;25(1):87–91. doi:10.1097/BOR.0b013e32835b13b6
18. Jayson GC, Kerbel R, Ellis LM, Harris AL. Antiangiogenic therapy in oncology: current status and future directions. *Lancet*. 2016;388 (10043):518–529.
19. Chen J, Ding X, Du W, Tang X, Yu WZ. Inhibition of corneal neovascularization by topical application of nintedanib in rabbit models. *Int J Ophthalmol*. 2021;14(11):1666–1673. doi:10.18240/ijo.2021.11.04
20. Spigel DR, Rubin MS, Gian VG, et al. Sorafenib and continued erlotinib or sorafenib alone in patients with advanced non-small cell lung cancer progressing on erlotinib: a randomized Phase II study of the Sarah Cannon Research Institute (SCRI). *Lung Cancer*. 2017;113:79–84. doi:10.1016/j.lungcan.2017.09.007
21. Demetri GD, van Oosterom AT, Garrett CR, et al. Efficacy and safety of sunitinib in patients with advanced gastrointestinal stromal tumour after failure of imatinib: a randomised controlled trial. *Lancet*. 2006;368(9544):1329–1338.
22. Ma D, Chen L, Shi J, et al. Pigment epithelium-derived factor attenuates angiogenesis and collagen deposition in hypertrophic scars. *Wound Repair Regen*. 2020;28(5):684–695. doi:10.1111/wrr.12828
23. Hu-Lowe DD, Zou HY, Grazzini ML, et al. Nonclinical antiangiogenesis and antitumor activities of axitinib (AG-013736), an oral, potent, and selective inhibitor of vascular endothelial growth factor receptor tyrosine kinases 1, 2, 3. *Clin Cancer Res*. 2008;14(22):7272–7283. doi:10.1158/1078-0432.CCR-08-0652
24. Gross-Goupil M, Francois L, Quivy A, Ravaud A. Axitinib: a review of its safety and efficacy in the treatment of adults with advanced renal cell carcinoma. *Clin Med Insights Oncol*. 2013;7:269–277. doi:10.4137/CMO.S10594
25. Morris DE, Wu L, Zhao LL, et al. Acute and chronic animal models for excessive dermal scarring: quantitative studies. *Plast Reconstr Surg*. 1997;100(3):674–681. doi:10.1097/00006534-199709000-00021
26. Li J, Wang J, Wang Z, et al. Experimental models for cutaneous hypertrophic scar research. *Wound Repair Regen*. 2020;28(1):126–144. doi:10.1111/wrr.12760
27. Lledo Riquelme M, Campos-Mollo E, Fernandez-Sanchez L. Topical axitinib is a potent inhibitor of corneal neovascularization. *Clin Exp Ophthalmol*. 2018;46(9):1063–1074. doi:10.1111/ceo.13333
28. Thompson CM, Sood RF, Honari S, Carrougher GJ, Gibran NS. What score on the Vancouver Scar Scale constitutes a hypertrophic scar? Results from a survey of North American burn-care providers. *Burns*. 2015;41(7):1442–1448. doi:10.1016/j.burns.2015.04.018
29. Wang D, Stockard CR, Harkins L, et al. Immunohistochemistry in the evaluation of neovascularization in tumor xenografts. *Biotech Histochem*. 2008;83(3–4):179–189. doi:10.1080/10520290802451085
30. Kim S, Choi TH, Liu W, Ogawa R, Suh JS, Mustoe TA. Update on scar management: guidelines for treating Asian patients. *Plast Reconstr Surg*. 2013;132(6):1580–1589. doi:10.1097/PRS.0b013e3182a8070c
31. Keating GM. Axitinib: a review in advanced renal cell carcinoma. *Drugs*. 2015;75(16):1903–1913. doi:10.1007/s40265-015-0483-x

32. Kwak DH, Bae TH, Kim WS, Kim HK. Anti-vascular endothelial growth factor (Bevacizumab) therapy reduces hypertrophic scar formation in a rabbit ear wounding model. *Arch Plast Surg*. 2016;43(6):491–497. doi:10.5999/aps.2016.43.6.491

33. Song Y, Yu Z, Song B, et al. Usnic acid inhibits hypertrophic scarring in a rabbit ear model by suppressing scar tissue angiogenesis. *Biomed Pharmacother*. 2018;108:524–530. doi:10.1016/j.biopha.2018.06.176

34. Ren HT, Hu H, Li Y, Jiang HF, Hu XL, Han CM. Endostatin inhibits hypertrophic scarring in a rabbit ear model. *J Zhejiang Univ Sci B*. 2013;14 (3):224–230. doi:10.1631/jzus.B1200077

35. Tan W, Jia W, Sun V, Mihm MC, Nelson JS. Topical rapamycin suppresses the angiogenesis pathways induced by pulsed dye laser: molecular mechanisms of inhibition of regeneration and revascularization of photocoagulated cutaneous blood vessels. *Lasers Surg Med*. 2012;44 (10):796–804. doi:10.1002/lsm.22101